Available online at www.sciencedirect.com
ScienceDirect
Journal of the European Ceramic Society 27 (2007) 4521–4527
www.elsevier.com/locate/jeurceramsoc

Effect of Ag on the microstructure and electrical properties of ZnO

Shu-Ting Kuo [a], Wei-Hsing Tuan [a,*], Jay Shieh [a], Sea-Fue Wang [b]

[a] *Department of Materials Science and Engineering, National Taiwan University, Taipei, Taiwan*
[b] *Department of Materials and Mineral Resources Engineering, National Taipei University of Technology, Taipei, Taiwan*

Received 7 October 2006; received in revised form 14 February 2007; accepted 23 February 2007
Available online 14 May 2007

Abstract

Various amounts of silver particles, 0.08–7.7 mol%, are mixed with zinc oxide powder and subsequently co-fired at 800–1200 °C. The effects of Ag addition on the microstructural evolution and electrical properties of ZnO are investigated. A small Ag doping amount (<0.76 mol%) promotes the grain growth of ZnO; however, a reversed trend in grain growth is observed for a relatively larger Ag addition (>3.8 mol%). It is evident that a tiny amount of Ag (~0.08 mol%) may dissolve into the ZnO lattice. High-resolution TEM observations give direct evidences on the segregation of Ag solutes at the ZnO grain boundaries. The grain boundary resistance of ZnO increases 35-fold with the presence of Ag solute segregates. The Ag-doped ZnO system exhibits a nonlinear electric current–voltage characteristic, confirming the presence of an electrostatic barrier at the grain boundaries. The barrier is approximately 2 V for a single grain boundary.
© 2007 Elsevier Ltd. All rights reserved.

Keywords: Microstructure-final; Electrical properties; Impedance; ZnO; Ag

1. Introduction

Zinc oxide (ZnO) is an n-type semiconductor with a wide band gap (3.437 eV at 2 K),[1,2] and has been used as the material for surge suppressors, gas sensors and transducers, etc.[3–6] For many electrical applications, silver and silver alloys are used as the electrode materials. In order to reduce the manufacturing cost, the electrodes are frequently co-fired with ZnO to elevated temperatures. ZnO and Ag may interact with each other during co-firing; however, such interaction has received relatively little attention in the literature.

In a study conducted by Fan and Freer,[7] the effects of 1000 ppm of Ag doping on the electrical properties of ZnO varistor compositions (i.e. ZnO mixed with Bi_2O_3, Sb_2O_3, Co_2O_3, Cr_2O_3, MnO_2 and B_2O_3) were studied. They found that both the grain and grain boundary resistances increase with the addition of Ag, and proposed that Ag^+ could substitute Zn^{2+} and acts as an acceptor in ZnO, expressed as

$$2Ag \xrightarrow{ZnO} 2Ag'_{Zn} + V_O^{\bullet\bullet} \quad (1)$$

Due to the formation of Ag acceptors, the grain resistance is increased. Fan and Freer also suggested that Ag^+ may behave like many other monovalent dopant ions (e.g. Na^+ and K^+) which have the ability to occupy both the lattice and interstitial sites (i.e. amphoteric dopants), expressed as

$$2Ag \xrightarrow{ZnO} Ag'_{Zn} + Ag_i^{\bullet} \quad (2)$$

They proposed that Ag'_{Zn} may occupy the grain boundary sites, and consequently, the grain boundary resistance is increased. The effects of Ag addition on the microstructural evolution of ZnO during sintering were not addressed in their study.

In a study conducted by Jose and Khadar,[8] nano-sized ZnO and Ag (5–30 wt.%) particles were mixed together, and the impedance spectrums of the green compacts were studied. Both the grain and grain boundary resistances of ZnO increase slightly with the addition of nano-sized Ag particles. Jose and Khadar suggested that the increase in the resistances is related to the presence of Ag particles at the grain boundaries and triple junctions of the nanocrystalline ZnO. In their study the specimens (i.e. green compacts) were not co-fired at an elevated temperature. A more intense Ag–ZnO interaction might be observed if a suitable heat treatment was applied.

* Corresponding author. Tel.: +886 2 2365 9800; fax: +886 2 2363 4562.
E-mail address: tuan@ccms.ntu.edu.tw (W.-H. Tuan).

0955-2219/$ – see front matter © 2007 Elsevier Ltd. All rights reserved.
doi:10.1016/j.jeurceramsoc.2007.02.215

In the present study, ZnO and Ag powders are mixed together. The Ag-doped ZnO specimens are then co-fired together to elevated temperatures. The effects of Ag on the microstructural evolution and electrical properties of ZnO are investigated.

2. Experimental procedure

Zinc oxide (>99.95% ZnO, $d_{50} = 1.2\ \mu m$) and Ag (>99.9% Ag, $d_{50} = 1.4\ \mu m$) powders were ball-milled together in ethyl alcohol for 4 h using zirconia media. The amount of Ag ranged from 0.08 to 7.7 mol% (i.e. 0.1–10 wt.%). The slurry was dried in a rotary evaporator to remove the alcohol, and then sieved through a #150 plastic mesh. The mixed powders were consolidated into discs of 10 mm diameter and 3 mm thickness at a uniaxial pressure of about 25 MPa. These sample discs were sintered at 800–1200 °C in air for 1 h, with the heating and cooling rates of 5 °C/min. The weight loss during sintering was minimal.

The densities of the specimens after sintering were determined by the Archimedes water immersion method. The relative densities were estimated by using 5.68 g/cm^3 for ZnO and 10.5 g/cm^3 for Ag.[9,10] X-ray diffractometry (XRD, PW1830, Philips Co., the Netherlands) was used for phase analysis. The XRD was operated at 35 kV and 20 mA with a scanning rate of 3° 2θ/min. The surfaces of the specimens submitted for XRD analysis were covered with a thin layer of silicon paste used as an external standard to calibrate the peak position. For microstructure observation, the specimens were ground with SiC abrasive papers first and then polished with Al_2O_3 particles. The polished surfaces were etched with dilute hydrochloric acid. The microstructures were observed by scanning electron microscopy (SEM). An in-house image analysis technique was used to determine the grain size and its distribution. Approximately, 400–500 grains were measured for each composition specimen. For transmission electron microscope (TEM) observation, the specimens were ground, dimpled and ion-milled to electron transparency. Ion milling was performed using a precision ion polishing system (Model 691, GATAN, USA) at an accelerating voltage of 5 kV and a milling angle of 5°. The TEM analysis was conducted using a field-emission TEM (TECNAI F30, FEI Co., the Netherlands) operated at 300 kV.

For impedance and current–voltage (I–V) measurements, the sintered specimen discs were lapped to ensure the parallelness of the two circular faces, onto which top and bottom circular Ag electrodes (area = 28 mm^2) were applied. The thickness of the lapped specimens was about 0.8 mm. Impedance spectroscopic measurements were carried out using an impedance analyzer (HP 4194 A, Hewlett-Packard Co., USA) over the frequency range from 100 Hz to 5 MHz at a signal level of 500 mV and a measurement temperature of 120 °C. The resistance of the specimen was determined from the real-axis intercepts of the fitted semicircle for the experimental data in the impedance spectrum. The I–V characteristics of the Ag-doped ZnO specimens were measured using a dc current method at currents ranging from 1 μA to 1 A.

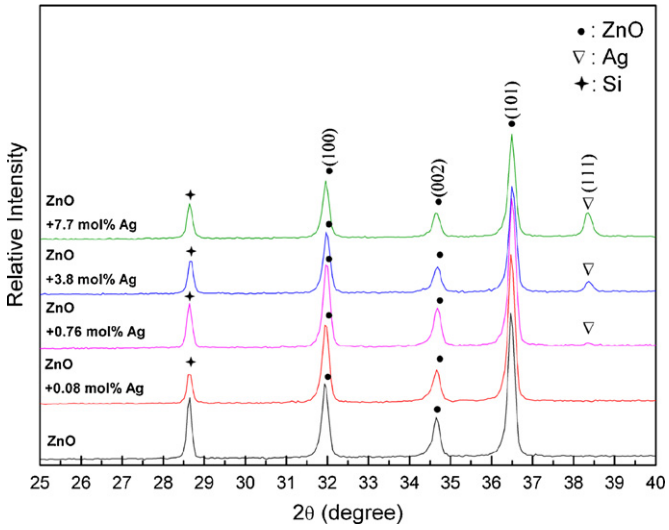

Fig. 1. XRD patterns of undoped and Ag-doped ZnO specimens sintered at 1200 °C for 1 h (specimen surface was coated with Si).

3. Results

3.1. Phase analysis

Fig. 1 shows the XRD patterns of the Ag-doped ZnO specimens sintered at 1200 °C for 1 h. The XRD patterns reveal that apart from ZnO and Ag, no other reaction phases are present. The Si peak is resulted from the coated Si paste. From the position of the Si peak, it is possible to calibrate the values of ZnO peaks.

It is evident that with increasing Ag doping level, the (1 0 0), (0 0 2) and (1 0 1) peaks of ZnO shift to the right progressively. Using these characteristic peaks, the lattice parameters a and c can be calculated by the following equation[11]:

$$d = \frac{a}{\sqrt{(4/3)(h^2 + k^2 + hk) + (a^2/c)l^2}} \quad (3)$$

In the above equation, h, k and l are the indices of the peak, and d is the planar distance. From the values of a and c, the unit cell volume can be determined. Fig. 2 clearly shows that the unit cell volume of ZnO decreases rapidly upon adding a small amount of Ag (<0.76 mol%). This decrease in the unit cell volume is halted when the doping amount of Ag is above 0.76 mol%.

3.2. Microstructure analysis

Fig. 3 shows the relative densities of the specimens as a function of sintering temperature. The sintered density increases slightly with Ag doping. The SEM micrographs of the Ag-doped ZnO specimens sintered at 1200 °C for 1 h are shown in Fig. 4. It is evident that most Ag inclusions locate at the boundaries and triple junctions of ZnO grains. Silver is a ductile metal, and grinding and polishing of specimen may deform the Ag inclusions, resulting in the appearance of a higher volume fraction of Ag.[12] The Ag content perceived from the SEM micrographs thus seems higher than the actual content.

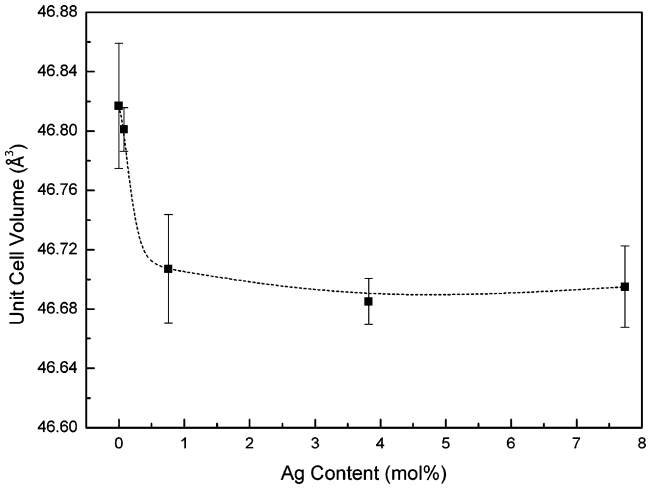

Fig. 2. Unit cell volume of ZnO as a function of Ag-doping content.

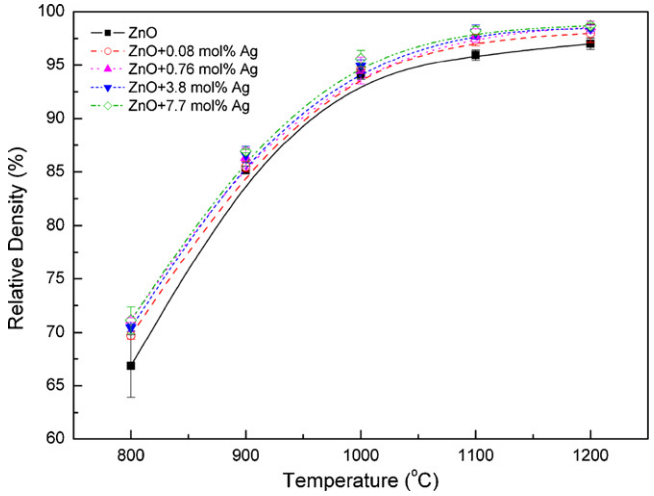

Fig. 3. Relative densities of undoped and Ag-doped ZnO specimens sintered at 800–1200 °C for 1 h.

The average and coefficient of variation of the grain size of the specimens are listed in Table 1. It is evident from Fig. 4 and Table 1 that a small amount of Ag (<0.76 mol%) promotes the grain growth of ZnO. However, a larger amount of Ag (e.g. 7.7 mol%) induces large inclusions and hinders the grain growth. Typical grain size distribution curves for the Ag-doped ZnO specimens are shown in Fig. 5. The mean size of ZnO grains is

Table 1
Mean size and size distribution of ZnO grains in undoped and Ag-doped ZnO specimens sintered at 1200 °C for 1 h

	Grain size (μm)	Coefficient of variation (%)[a]
Undoped ZnO	7.5 ± 4.1	55
ZnO + 0.08 mol% Ag	7.2 ± 2.8	39
ZnO + 0.76 mol% Ag	10.4 ± 4.1	39
ZnO + 3.8 mol% Ag	7.9 ± 3.4	43
ZnO + 7.7 mol% Ag	5.7 ± 2.4	42

[a] Standard deviation/mean value of grain size.

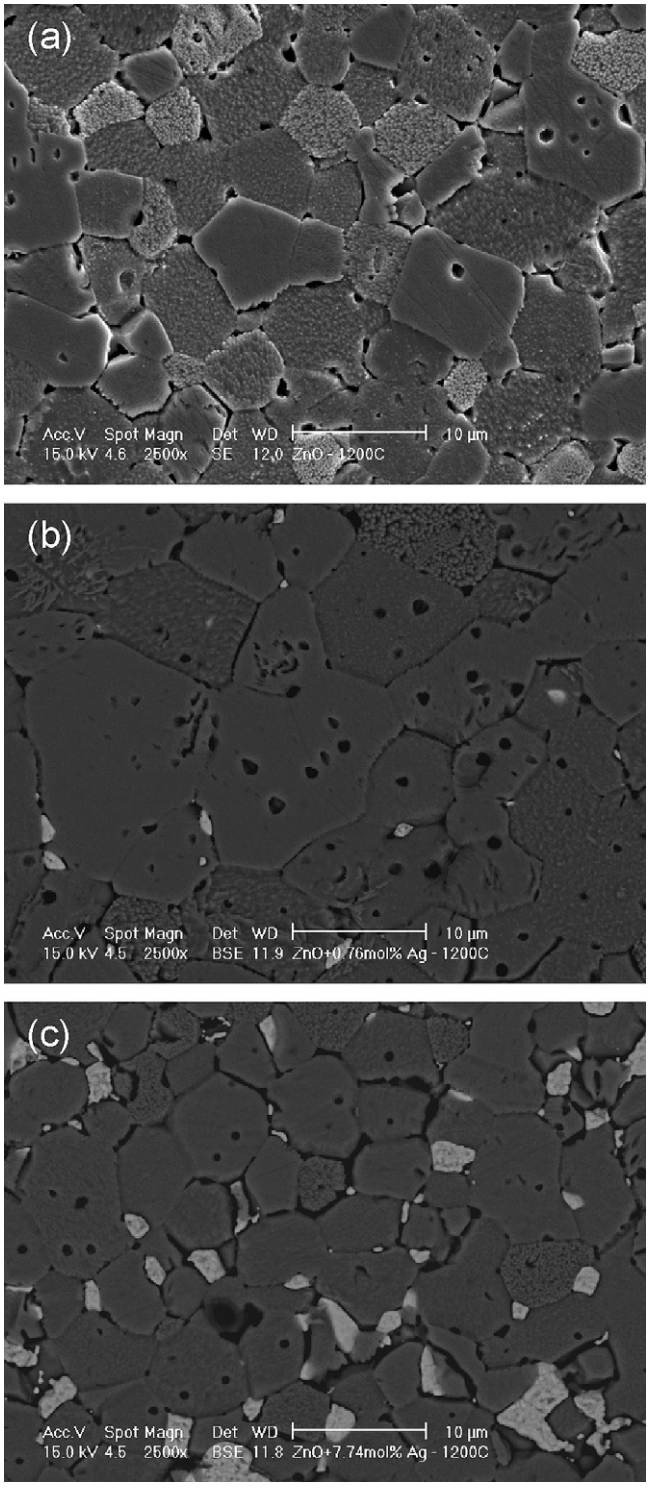

Fig. 4. SEM micrographs of (a) undoped, (b) 0.76 mol% Ag-doped, and (c) 7.7 mol% Ag-doped ZnO specimens sintered at 1200 °C for 1 h.

strongly dependent on the amount of Ag doping. Furthermore, the addition of Ag noticeably reduces the scattering of grain size.

A TEM image of an Ag inclusion at the triple junction of ZnO grains is shown in Fig. 6; the corresponding energy-dispersive X-ray spectrometry (EDX) patterns are also shown. The spot size of the electron beam for the TEM-EDX analysis is 6 nm. The TEM specimen is of 0.76 mol% of Ag doping, an amount which

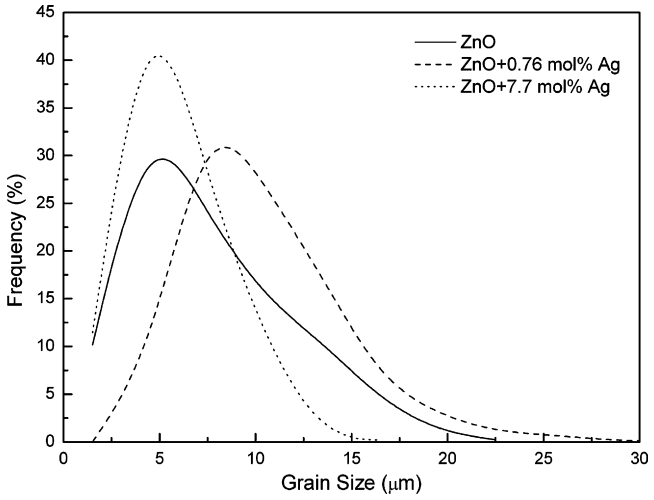

Fig. 5. Grain size distributions of undoped and 0.76 and 7.7 mol% Ag-doped ZnO specimens sintered at 1200 °C for 1 h.

is slightly higher than the solubility determined by the XRD analysis. The Ag contents in positions 1, 2 and 3 shown in the TEM image are 92, 2 and close to 0 at%, respectively. The EDX patterns show that at position 2, which is at a grain boundary 200 nm away from the Ag inclusion, a small Ag signal is still detected (see Fig. 6c). In contrast, position 3, which is within the ZnO grain and 50 nm away from the Ag inclusion, exhibits almost no Ag signal (see Fig. 6d). The TEM-EDX analysis gives direct evidences on the segregation of Ag solutes at the ZnO grain boundaries.

3.3. Electrical properties

Fig. 7 shows the impedance spectrums of the Ag-doped ZnO specimens. The resulting resistances of the specimens calculated from their spectrums are listed in Table 2. The addition of Ag reduces the grain resistance of ZnO, regardless the doping percentage. In contrast, the grain boundary resistance increases 35-fold to 8800 kΩ when a tiny amount of Ag, 0.08 mol%, is added. Further increasing the Ag doping level lowers the grain boundary resistance. When 7.7 mol% of Ag is added, the measured grain boundary resistance is 550 kΩ, still higher than that of pure ZnO.

Fig. 8 shows the *I–V* curves for the Ag-doped ZnO specimens. An approximate linear relationship between current density and electric field is observed for the pure ZnO specimen, indicating a semiconductor characteristic. In contrast, a nonlinear *I–V* relationship, characterized by a threshold electric field at which the current density spikes up, is observed for the Ag-doped ZnO specimens.

Table 2
Grain and grain boundary resistances of undoped and Ag-doped ZnO specimens sintered at 1200 °C for 1 h

	Grain resistance (Ω)	Grain boundary resistance (kΩ)
Undoped ZnO	370	250
ZnO + 0.08 mol% Ag	60	8800
ZnO + 0.76 mol% Ag	130	2400
ZnO + 3.8 mol% Ag	20	2900
ZnO + 7.7 mol% Ag	200	550

4. Discussion

4.1. Solubility of Ag in ZnO

To determine a minute solubility in ceramics by using XRD technique is a challenging task. An external standard, Si powder, is applied to coat onto the specimen before the XRD measurement. The Si peak is then used to calibrate the two values of the ZnO peaks. This technique has been well received by many research groups. For example, Kim et al. used such technique to determine the lattice parameters of HfO_2 and ZrO_2 crystals.[13] Their results had demonstrated that accuracy of the technique could be as high as 0.0001 nm. Therefore, the XRD technique together with Si internal standard employed in the present study is a reliable and accurate technique. By using such technique, the solubility of Ag in ZnO can thus be determined.

The XRD patterns indicate that the solubility of Ag in ZnO is between 0.08 and 0.76 mol% (see Fig. 1). The SEM image shown in Fig. 4b also suggests a solubility less than 0.76 mol%. Results from the XRD and TEM analyses suggest that no chemical reaction takes place between Ag and ZnO. However, the volume of ZnO unit cell decreases as a small amount of Ag (<0.76 mol%) is added. This implies that a minute amount of Ag is dissolved into the ZnO lattice after co-firing at 1200 °C. The size of Ag^+ ion (0.122 nm) is larger than that of Zn^{2+} ion (0.088 nm),[14] and therefore the level of substitution of Zn by Ag is expected to be quite low—about 0.08 mol% or slightly higher as indicated by the XRD test. Based on the TEM observation, most Ag solutes tend to segregate at the grain boundaries of ZnO. When the amount of Ag doping is less than 0.76 mol%, the presence of Ag promotes the densification and grain growth of ZnO. Furthermore, the scattering of ZnO grain size is reduced with the addition of Ag. In other words, the Ag solutes act as a microstructure stabilizer to the ZnO grains. The vapor pressure of Ag is relatively high at elevated temperatures,[15] and thus Ag vapor is readily transported during sintering through the pore channels within the ZnO powder compact. Such a vapor transport mechanism is essential to the distribution of a second phase (Ag in this case) especially when its amount is low.[16]

4.2. Role of Ag solutes

Due to the charge difference between Ag^+ and Zn^{2+}, the substitution of Zn by Ag at the lattice sites would result in the formation of Ag acceptors, as suggested by Eq. (1). The formation of acceptors is usually accompanied with an increase in grain resistance.[7] However, the decrease in grain resistance with Ag doping observed in the present study rules out this mechanism (see Table 2). This decrease in grain resistance is likely to be contributed mainly from the formation of oxygen vacancies with Ag doping. The increase in oxygen vacancy concentration promotes the densification of ZnO grains (see Fig. 3). The

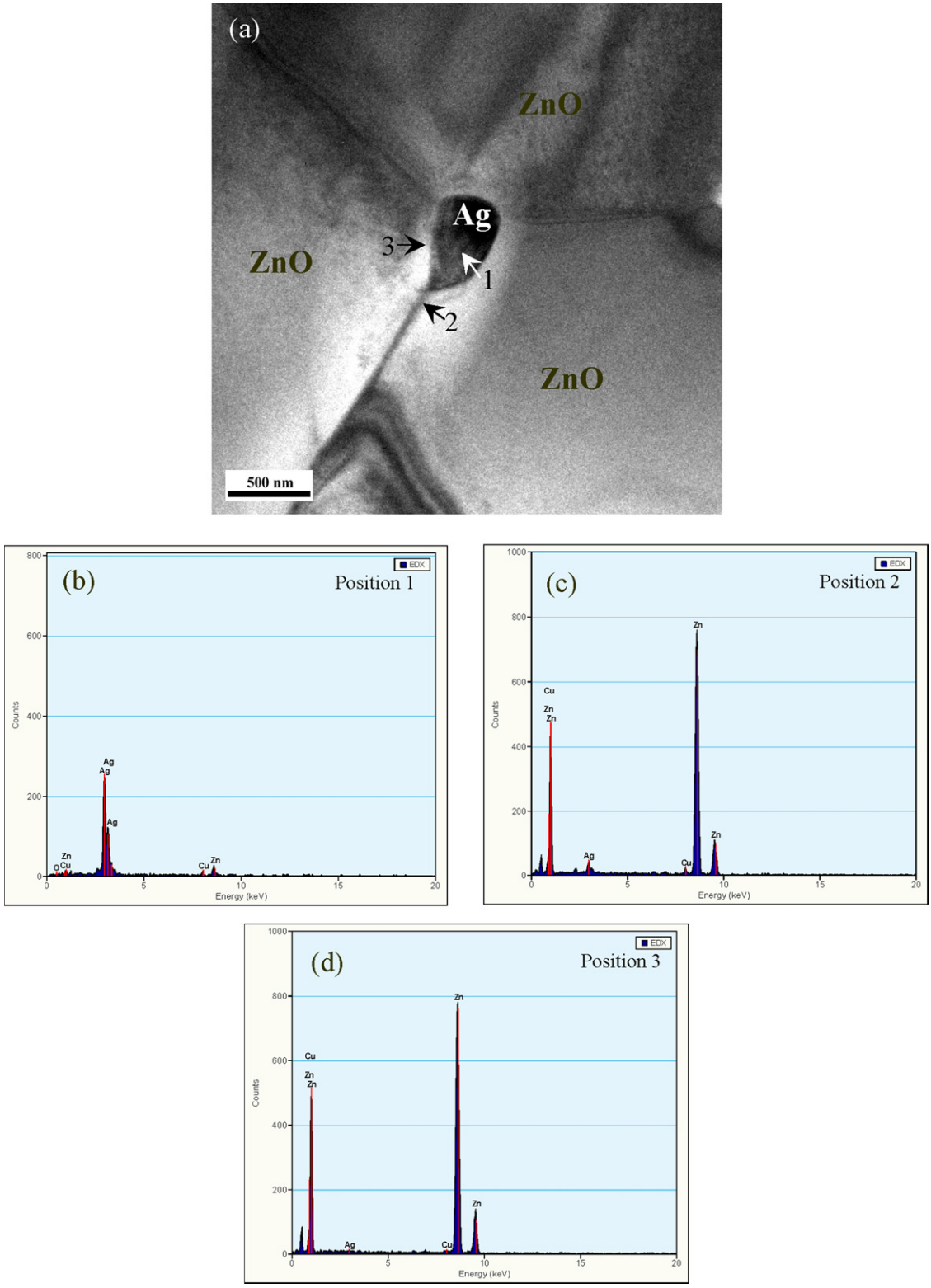

Fig. 6. (a) TEM image of an Ag inclusion in the 0.76 mol% Ag-doped ZnO specimen. The corresponding EDX patterns for positions 1, 2 and 3 in the TEM image are shown in (b), (c) and (d), respectively.

decrease in grain resistance is minor; thus, an increase in free electron concentration is not likely.

Typically the increase in density enhances the grain growth rate. Furthermore, the radius of Ag^{+} is much larger than that of Zn^{2+}; the segregation of Ag ions may hence induce considerable disorder or distortion near the grain boundaries.[17] Such disorder may provide routes or spaces for fast mass transportation. The ZnO grains thus grow faster due to the presence of Ag solutes

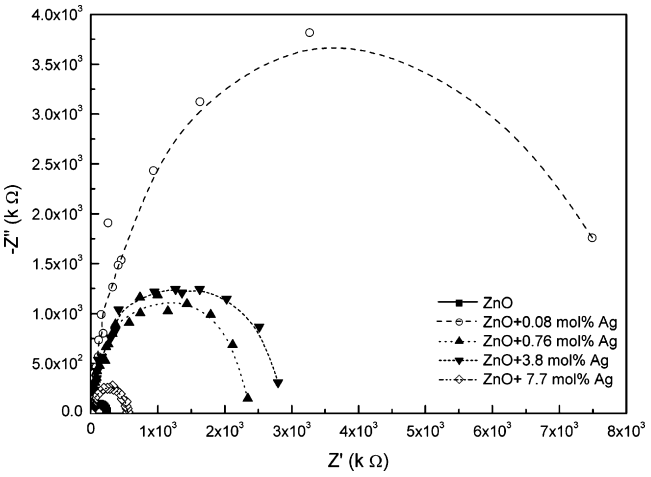

Fig. 7. Impedance spectrums of undoped and Ag-doped ZnO specimens sintered at 1200 °C for 1 h (spectrums were measured at 120 °C).

near the grain boundaries. This is likely the main reason why the grain size of the Ag-doped ZnO specimens with low Ag contents is large.

The grain boundary resistance of ZnO increases one order of magnitude after the addition of a very small amount of Ag dopant. It suggests the presence of Ag ions at the grain boundary. Due to the difference of ionic charge and radius between Zn^{2+} and Ag^{+}, the segregation of Ag at the grain boundary of ZnO is preferred. The Ag concentration at grain boundary is much higher than 0.08 mol% (see Fig. 6c). Such segregation may establish a space charge zone near the grain boundary.[18] Due to the presence of Ag dopant in the lattice, the XRD–ZnO peaks are shifted.

Previous studies have found that many monovalent dopants, such as K^{+} and Na^{+}, act as amphoteric dopants.[19,20] In the present study, Ag^{+} is likely to act as an amphoteric dopant and occupy both the lattice and interstitial sites since Ag solutes are not acceptors in ZnO. Ag^{+} would preferentially choose to sit in the vicinity of grain boundaries due to its large ionic radius.

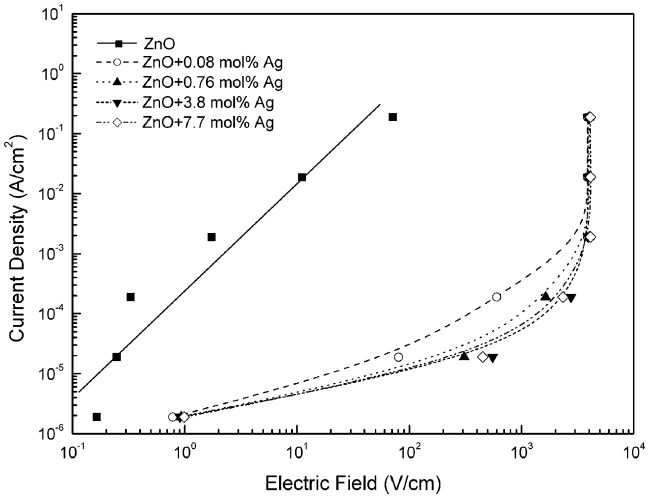

Fig. 8. *I–V* curves for undoped and Ag-doped ZnO specimens sintered at 1200 °C for 1 h.

The presence of Ag^{+} that segregates at the grain boundaries establishes an electrostatic barrier against the movement of electrons. A nonlinear *I–V* characteristic is thus observed for the Ag-doped ZnO specimens. From Fig. 8, the electrostatic barrier is about several thousand volts per one centimeter. By dividing with the average grain size (see Table 1), the electrostatic barrier of one-grain boundary is approximately 2 V.

4.3. Role of Ag inclusions

The solubility of Ag in ZnO is low. For Ag contents higher than 0.76 mol%, a large number of Ag inclusions are left at the grain boundaries and grain triple junctions after co-firing. The growth of ZnO grains is hindered when more than 3.8 mol% of Ag is added. A relatively large amount of Ag inclusions reduces not only the mean grain size but also the grain size scattering. In the present study, the number of Ag inclusions produced at high doping amounts is not enough to pin all grain boundaries (see Fig. 4c). The ability of Ag inclusions to reduce the size scattering of ZnO grains is therefore similar to that of Ag solute segregates.

The formation of Ag–ZnO interfaces due to Ag inclusions increases the resistance of the Ag-doped ZnO system. The grain boundary resistance of the ZnO–0.08 mol% Ag specimen is the highest among the Ag-doped ZnO specimens, indicating that the Ag solute segregates can induce a much higher resistance. The grain boundary resistance decreases with increasing Ag content, suggesting that a decrease in the distance between Ag inclusions reduces the grain boundary resistance.

5. Conclusion

The effects of Ag addition on the microstructural evolution and electrical properties of ZnO have been investigated. It is found that a small amount of Ag, around 0.08 mol% or slightly higher, can dissolve into the ZnO lattice. The presence of Ag solutes increases the rates of densification and grain growth. The Ag solutes tend to segregate at the grain boundaries, and this segregation of Ag^{+} ions significantly raises the grain boundary resistance and establishes an electrostatic barrier against electron transportation. The barrier is approximately 2 V for a single grain boundary.

Acknowledgement

Financial support is provided by the National Science Council, Taiwan, under the contract number NSC94-2216-E-002-008.

References

1. Gupta, T. K., Application of zinc oxide varistors. *J. Am. Ceram. Soc.*, 1990, **73**(7), 1817–2177.
2. Zhou, Z., Kato, K., Komaki, T., Yoshino, M., Yukawa, H., Morinaga, M. *et al.*, Effects of dopants and hydrogen on the electrical conductivity of ZnO. *J. Eur. Ceram. Soc.*, 2004, **24**, 139–149.
3. Jose, J. and Khadar, M. A., Impedance spectroscopic analysis of ac response of nanophase ZnO and ZnO–Al_2O_3 nanocomposites. *Nanostruct. Mater.*, 1999, **11**(8), 1091–1099.

4. Singhal, M., Chhabra, V., Kang, P. and Shah, D. O., Synthesis of ZnO nanoparticles for varistor application using Zn-substituted aerosol OT microemulsion. *Mater. Res. Bull.*, 1997, **32**(2), 239–247.
5. Lin, H. M., Tzeng, S. J., Hsiau, P. J. and Tsai, W. L., Electrode effects on gas sensing properties of nanocrystalline zinc oxide. *Nanostruct. Mater.*, 1998, **10**(3), 465–477.
6. Srikant, V., Sergo, V. and Clarke, D. R., Epitaxial aluminum-doped zinc oxide thin films on sapphire. II. Defect equilibria and electrical properties. *J. Am. Ceram. Soc.*, 1995, **78**(7), 1935–1939.
7. Fan, J. and Freer, R., The roles played by Ag and Al dopants in controlling the electrical properties of ZnO varistors. *J. Appl. Phys.*, 1995, **77**(9), 4795–4800.
8. Jose, J. and Khadar, M. A., Role of grain boundaries on the electrical properties of ZnO–Ag nanocomposites: an impedance spectroscopic study. *Acta Mater.*, 2001, **49**, 729–735.
9. JCPD 05-0664, Inter. Center for Diffraction. Data, JCPDs, Penn, USA, 1983.
10. JCPD 04-0783, Inter. Center for Diffraction. Data, JCPDs, Penn, USA, 1983.
11. Cullity, B. D. and Stock, S. R., In *X-ray diffraction*. 3rd ed. Prentice-Hall, New Jersey, 2001. p. 619.
12. Tuan, W. H. and Chen, W. R., The mechanical properties of Al_2O_3–ZrO_2–Ag composites. *J. Am. Ceram. Soc.*, 1995, **78**(2), 465–469.
13. Kim, D.-J., Hyun, S.-H., Kim, S.-G. and Yashima, M., Effective ionic radius of Y^{3+} determined from lattice parameters of fluorite-type HfO_2 and ZrO_2 solid solution. *J. Am. Ceram. Soc.*, 1994, **77**(2), 597–599.
14. Weast Robert, C., *Handbook of chemistry and physics*, 70th ed. CRC, Boca Raton, Fl, 1989–1990, p. B-68.
15. Chen, C. Y. and Tuan, W. H., Effect of silver on the sintering and grain-growth behavior of barium titanate. *J. Am. Ceram. Soc.*, 2000, **83**(12), 2988–2992.
16. Luo, J., Wang, H. and Chiang, Y. M., Origin of solid-state activated sintering in Bi_2O_3-doped ZnO. *J. Am. Ceram. Soc.*, 1999, **82**(4), 916–920.
17. MacLaren, I., Cannon, R. M., Gulgun, M. A., Voytovych, R., Popescu-Pogrion, N., Scheu, C. *et al.*, Abnormal grain growth in alumina: synergistic effects of yttria and silica. *J. Am. Ceram. Soc.*, 2003, **86**(4), 650–659.
18. Chiang, Y.-M. and Takagi, T., Grain-boundary chemistry of barium titanate and strontium titanate. I. High-temperature equilibrium space charge. *J. Am. Ceram. Soc.*, 1990, **73**(11), 3278–3285.
19. Gupta, T. K. and Miller, A. C., Improved stability of the ZnO varistor via donor and acceptor doping at the grain boundary. *J. Mater. Res.*, 1988, **3**(4), 745–754.
20. Blinks, D. J. and Grimes, R. W., Incorporation of monovalent ions in ZnO and their influence on varistor degradation. *J. Am. Ceram. Soc.*, 1993, **76**(9), 2370–2372.